Pharm Res (2014) 31:1946–1957
DOI 10.1007/s11095-014-1296-4

RESEARCH PAPER

Coformer Screening Using Thermal Analysis Based on Binary Phase Diagrams

Hiroyuki Yamashita • Yutaka Hirakura • Masamichi Yuda • Katsuhide Terada

Received: 8 August 2013 / Accepted: 31 December 2013 / Published online: 13 February 2014

ABSTRACT

Purpose The advent of cocrystals has demonstrated a growing need for efficient and comprehensive coformer screening in search of better development forms, including salt forms. Here, we investigated a coformer screening system for salts and cocrystals based on binary phase diagrams using thermal analysis and examined the effectiveness of the method.

Methods Indomethacin and tenoxicam were used as models of active pharmaceutical ingredients (APIs). Physical mixtures of an API and 42 kinds of coformers were analyzed using Differential Scanning Calorimetry (DSC) and X-ray DSC. We also conducted coformer screening using a conventional slurry method and compared these results with those from the thermal analysis method and previous studies.

Results Compared with the slurry method, the thermal analysis method was a high-performance screening system, particularly for APIs with low solubility and/or propensity to form solvates. However, this method faced hurdles for screening coformers combined with an API in the presence of kinetic hindrance for salt or cocrystal formation during heating or if there is degradation near the metastable eutectic temperature.

Conclusions The thermal analysis and slurry methods are considered complementary to each other for coformer screening. Feasibility of the thermal analysis method in drug discovery practice is ensured given its small scale and high throughput.

KEY WORDS binary phase diagram · cocrystal · coformer screening · thermal analysis

H. Yamashita (✉) · Y. Hirakura · M. Yuda
Analysis and Pharmacokinetics Research Labs, Astellas Pharma Inc.
21, Miyukigaoka, Tsukuba, Ibaraki 350-8585, Japan
e-mail: hiroyuki.yamashita@astellas.com

H. Yamashita · K. Terada
Faculty of Pharmaceutical Science, Toho University, 2-2-1, Miyama
Funabashi, Chiba 274-8510, Japan

INTRODUCTION

Increasing attention has been focused on cocrystals as a development form in the pharmaceutical industry given their potential, like salts, to improve the physicochemical properties of active pharmaceutical ingredients (APIs), including solubility (1–3), physical stability (4,5), mechanical properties (6,7), and bioavailability (8). While salts are often used as a development form, some APIs under development as SGLT2 inhibitors for diabetes, such as ipragliflozin (L-proline cocrystal) (9) and ertugliflozin (L-pyroglutamic acid cocrystal) (10), are in cocrystal form. The pharmaceutical industry generally defines cocrystals as a crystal comprised of one API and one or more unique solid coformer associated by reversible "non-ionic" binding (11,12), whereas a salt is defined as a crystal associated by reversible "ionic" binding. Notably, a larger selection of coformers exists as cocrystals than as salts, because the former requires no dissociable groups. As such, since the volume of cocrystal screening is increasing to surpass that of salt screening, efficient methods for the screening of cocrystals are becoming increasingly important.

Cocrystal screening is generally conducted using slurry solutions (13–15), ultrasound crystallization (16), evaporation (17), or supercritical fluids (18). The above are all solution methods, which may involve issues with precipitating the API or conformer and preventing cocystal formation when the difference in solubility between the two components is large (13). Further, these methods tend to require a large number of experiments in light of the diversity of solvents required, a necessity not desirable with respect to green chemistry. As an alternative, screening methods using the solid state, such as neat grinding (19,20), solvent drop grinding (20–22), and heat-induced crystallization (8,23), have been reported; however, these approaches typically require a large amount of sample and are not high-throughput, highlighting the need for a small-scale, high-throughput cocrystal screening system using solid state.

We previously reported the detection of cocrystal formation based on binary phase diagrams (Fig. 1) using thermal analysis (24). When a physical mixture consisting of two components capable of cocrystal formation is heated using differential scanning calorimetry (DSC), an exothermic peak associated with the cocrystal formation is detected immediately after an endothermic peak. In some mixtures, several endothermic peaks may be detected with metastable eutectic melting, eutectic melting, and cocrystal melting. In contrast, for a physical mixture of two components incapable of cocrystal formation heated using DSC, only a single endothermic peak associated with eutectic melting is detected. These results indicate that cocrystal screening is feasible based on whether or not an exothermic peak exists and/or whether or not several endothermic peaks exist. Importantly, because the phase diagram of a salt crystal is reported to be similar to that of a cocrystal (25), this strategy of screening using phase diagrams is applicable to screening of either crystal type. Therefore, initially, no distinction between a salt or cocrystal is necessary in any process, including experimentation and data interpretation. Further, the structure of the phase diagram is qualitatively the same for cocrystals (salts) of different molar ratios. When an API and a stoichiometric (1:1) coformer are heated using standard procedures, metastable eutectic melting occurs with heat absorption at the metastable eutectic temperature, and cocrystallization (salt formation) follows with heat generation irrespective of the stoichiometry of the crystal formed. In short, heat generation can be observed independent of the stoichiometry of the cocrystal (salt) structure if the mixture is capable of cocrystal (salt) formation. These characteristics enable us to create a versatile coformer screening system.

Coformer screening of salts and cocrystals based on binary phase diagrams using thermal analysis should prove more useful than other conventional screening systems, due to its high-throughput style and small scale, its independence from issues of solubility in solvent and preferences for solvents in crystallization, and its green chemistry aspect. To demonstrate the usefulness of this approach, we conducted coformer screening using DSC of indomethacin (IND) and tenoxicam (TEN) as models of API (Fig. 2) and 42 kinds of coformers (Table I). Both IND and TEN are clinically-available nonsteroidal anti-inflammatory drugs for which salt and cocrystal forms have been reported and physicochemical information is available (15,22,26–29). Before coformer screening is conducted, attention should be paid to the choice of the coformers based on their safety information as well as physicochemical properties, which are publically available for the 42 coformers (30–32).

Here, to directly confirm salt crystal or cocrystal formation and prevent erroneous conclusions, physical mixtures with either or both exothermic or plural endothermic peaks on DSC curves were further analyzed using X-ray DSC. In addition, we also conducted coformer screening of IND and TEN via a conventional slurry method and compared the results obtained using the thermal analysis method, slurry method, and data from other studies (15,22).

MATERIALS AND METHODS

Materials

IND and TEN were purchased from Sigma Aldrich (St. Louis, MO, USA). Saccharin, urea, citric acid, L-arginine, L-aspartic acid, L-glutamic acid, L-lysine, meglumine, benzoic acid, fumaric acid, *o*-aminobenzoic acid, and *p*-hydroxybenzoic acid were obtained from Wako Pure Chemical Industries (Osaka, Japan). Nicotinamide and adipic acid were purchased from Nacalai Tesque (Kyoto, Japan). 1-hydroxy-2-naphthoic

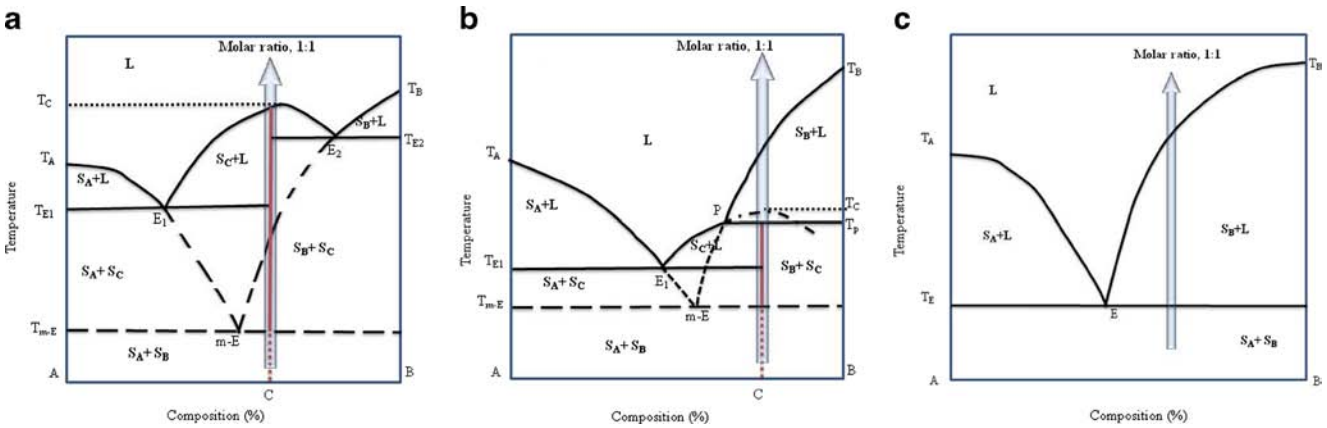

Fig. 1 Binary phase diagrams of combinations capable of cocrystal formation. (**a**) Congruent melting system, (**b**) incongruent melting system and (**c**) incapable of cocrystal formation (24). *L* liquid, S_A solid of component A, S_B solid of component B, S_C cocrystal, *E* eutectic point, *m-E* metastable eutectic point, *P* peritectic point, $T_{m\text{-}E}$ metastable eutectic temperature, T_E eutectic temperature, T_P peritectic temperature, T_A melting temperature of component A, T_B melting temperature of component B, T_C melting temperature of cocrystal.

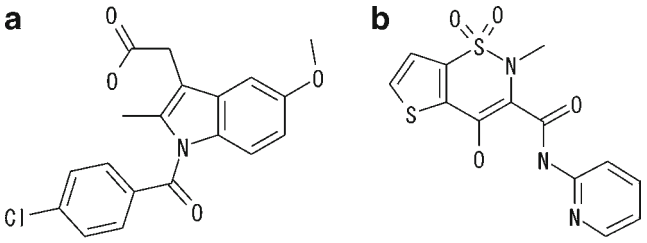

Fig. 2 Chemical structures of indomethacin (**a**) and tenoxicam (**b**).

acid, aceturic acid, choric acid, galactaric acid, gentisic acid, L-ascorbic acid, L-pyroglutamic acid, sorbic acid, and stearic acid were purchased from Tokyo Chemical Industry Co., Ltd. (Tokyo, Japan). All other compounds and solvents were of analytical grade, obtained from Kanto Chemical Co., Inc. (Tokyo, Japan), and used as received.

Automated Powder Dispensing

Core Module 3 (CM3) systems (Freeslate, Sunnyvale, CA, USA) were used for automatic powder dispensing. Ten milligrams of an API (IND or TEN) and stoichiometric (1:1) coformers were dispensed with an accuracy of ±5% into separate 1.2-mL microtubes that had been placed in a 96-well-type cassette for ball mill grinding.

Ball Mill Grinding

High-throughput grinding was conducted using a ball mill instrument (TissueLyser II) and the aforementioned 1.2-mL collection microtubes (QIAGEN, Tokyo, Japan). A 3-mm ball made from zirconia was placed into each microtube after powder dispensing. The grinding period and frequency were 5 min and 20/s, respectively.

Differential Scanning Calorimetry (DSC)

Thermal analysis of physical mixtures was performed using a TA Q1000 DSC instrument that included a refrigerated cooling system (TA Instruments, New Castle, DE, USA). Temperature calibration was carried out using the indium metal standard supplied with the instrument. Samples were weighed out (1.5–2.5 mg) in aluminum pans and analyzed from 25 to 250°C at heating rates of 5 and 30°C/min using a similar empty pan as a reference. An inert atmosphere was maintained in the calorimeter by purging nitrogen gas at a flow rate of 50 mL/min.

X-ray DSC

Simultaneous measurement of powder X-ray diffraction and DSC was carried out using a SmartLab system (X-ray wavelength: 0.154 nm Cu Kα source, voltage: 45 kV, current: 200 mA) with a DSC attachment and a D/Tex Ultra adapted as a detector (Rigaku, Tokyo, Japan). Physical mixtures were weighed out (1.5–2.0 mg) in aluminum pans and analyzed from 25 to 250°C at a heating rate of 2°C/min using a similar empty pan as a reference. X-ray diffraction data were collected at a scan rate of 20°/min over a 2θ range of 8° to 28°. Physical mixtures of IND and nicotinamide and of TEN and glycolic acid were also analyzed using a heating rate of 1°C/min.

Database

DSC and X-ray DSC patterns of each compound were collected prior to screening. A database of peaks appearing on DSC traces and patterns obtained with X-ray DSC analysis of single compounds, including IND and TEN, was created to compare with results obtained using a physical mixture. Screening hits were determined by referencing this database.

Salt and Cocrystal Screening by Slurry Method

IND or TEN (5 mg) and stoichiometric (1:1) coformers were dispensed into 1-mL vials using a powder dispenser of CM3. Crystallization solvents (0.2 mL) were also dispensed into each 1-mL vial using a liquid dispenser of CM3 after powder dispensing. Eight kinds of solvents—namely acetonitrile, ethanol, 1,4-dioxane, 2-butanone, ethyl acetate, toluene, 2-propanol/water (9:1), and tetrahydrofuran/water (9:1)—were used as crystallization solvents. These solvents were chosen based on their chemical and physicochemical diversity, safety consideration according to the ICH standard, and the ease of handling in terms of the boiling point. Vials were stirred for 24 h at 30°C using a stirring bar placed into each vial. Solvents were removed from the vials using comb paper and dried under reduced pressure for 3 h at 50°C using a vacuum drying oven, DP43 (Yamato Scientific Co., Ltd., Tokyo, Japan). Collected powders were characterized by powder X-ray diffraction (PXRD) and DSC patterns. The PXRD patterns (X-ray wavelength, 0.154 nm Cu Kα radiation; voltage, 40 kV; current, 40 mA) of the powders were measured using D8 Discover with GADDS (Bruker AXS, Yokohama, Japan). Data collection was conducted for 3 min per sample over a 2θ range of 5° to 26° through a 2-dimentional detector and a collimator of 0.3-mm pinhole. DSC patterns were measured from 25 to 250°C at a heating rate of 30°C/min using the above-cited instrument.

Thermogravimetric Analysis (TGA)

TGA of a physical mixture of TEN and glycolic acid was performed using a TA Q500 TGA instrument (TA Instruments, New Castle, DE, USA). Approximately 4 mg of sample was loaded into a platinum pan and heated to 200°C

Table I Coformers Used in this Study and their Safety Information

No.	Name	Handbook of Pharmaceutical salts Class[a]	GRAS Type[b]	Pharmaceutical salts and Co-crystals[c]	Melting point (°C)
1	(+)-Camphoric acid	2			186–189
2	1-Hydroxy-2-Naphthoic acid	2			195
3	Aceturic acid (N-acetylglycine)	1			207–209
4	Adipic acid	1			151–154
5	Benzoic acid	2	1		122
6	Cholic acid		1	✓	200
7	Citric acid	1	1	✓	153
8	D-Glucuronic acid	1			165
9	Erythorbic acid		1		169–172
10	Fumaric acid	1		✓	287–302
11	Galactaric acid (Mucic acid)	1			220–225
12	Gentisic acid (2,5-dihydroxybenzoic acid)	2			199–200
13	Glutaric acid	1		✓	97–98
14	Glycolic acid	1			79
15	Hippuric acid	1			191
16	Inositol		1		225
17	L-Arginine	1			238
18	L-Ascorbic acid	1	1	✓	190–192
19	L-Aspartic acid	1			270–271
20	L-Glutamic acid	1	2	✓	199–200
21	L-Lysine	1			215
22	L-Malic acid	1	1	✓	100
23	L-Pyroglutamic acid	2			162
24	L-Tartaric acid	1	1	✓	168–170
25	Maleic acid	1		✓	131–139
26	Malonic acid	2		✓	135
27	Meglumine (N-methyl-Glucamine)	1			128–129
28	Nicotinamide		1	✓	130
29	Nicotinic acid	2			236
30	*o*-Aminobenzoic acid (Anthranilic acid)			✓	146–148
31	Orotic acid	2			345–346
32	*p*-Aminobenzoic acid			✓	187–189
33	para-Toluenesulfonic acid	2			106–107
34	*p*-Hydroxybenzoic acid (4-Hydroxybenzoic acid)			✓	215–217
35	Saccharin	3		✓	228
36	Sebacic acid	1			134
37	Sorbic acid		1	✓	135
38	Sorbitol		1		95
39	Stearic acid (Octadecanoic acid)	1		✓	70–71
40	Succinic acid	1	1	✓	188
41	Tromethamine	2		✓	171
42	Urea		1	✓	132

[a] Numbers indicate the degree of safety shown in (32). Class 1: Salt formers that are of unrestricted use because they are physiologically ubiquitous ions occurring as intermediate metabolites in biochemical pathways. Class 2: Salt formers that are considered not to naturally occur, but during their profuse application have shown low toxicity and good tolerability. Class 3: Salt formers might be interesting under particular circumstances in order to achieve special effects such as ion-pair formation, or for solving particular problems

[b] Numbers indicate the degree of availability and hazard as food shown in (31). Type 1: No available evidence demonstrates or suggests reasonable grounds to suspect a hazard to the public when used at current or expected future levels. Type 2: No evidence available on substance that demonstrates a hazard to the public when used at current levels. However, without additional data, whether or not a significant increase in consumption would constitute a dietary hazard cannot be determined

[c] Check marks indicate the enrollment of safety information in reference book (30)

at a rate of 5 or 30°C/min. Measurements were carried out under a nitrogen purge with a flow rate of 50 mL/min. Temperature calibration was carried out using standard nickel.

Simplified Solubility Test

Two milligrams of an API was weighed out into a 10-mL vial. A predetermined amount of solvent was added stepwise to the

vial, which was subsequently sonicated for 5 s using a water-bath type ultrasonic device (SONO CLEANER 100Z, KAIJO CORPORATION, Tokyo, Japan). When powder had disappeared from view on macroscopic observation, solvent addition was terminated, and solubility was calculated from the total amount of added solvent.

Definition of Salt and Cocrystal

The general definitions of salts and cocrystals have been the subject of dispute (33,34). In this study, crystals of an API-coformer complex were defined as a salt or cocrystal based on ΔpKa (pKa [base]—pKa [acid]), with a complex defined as "salt" if ΔpKa was at least 1 and "cocrystal" if ΔpKa was less than 1. The pKa of each compound was calculated using ACD/Labs 2012 (Advanced Chemistry Development, Inc., Tronto, Ontario, Canada).

RESULTS AND DISCUSSION

Coformer Screening Using Thermal Analysis on Indomethacin

Coformer screening based on thermal analysis was conducted using IND as a model API and 42 kinds of coformers. Exothermic peaks were detected on the DSC curves of physical mixtures of IND and L-arginine, L-lysine, or saccharin, and plural endothermic peaks were found on those of IND and either *o*-aminobenzoic acid or *p*-toluenesulfonic acid (Table II). The DSC curves of the physical mixtures of IND and meglumine, sorbic acid, or tromethamine had a broad endothermic peak. This peak appeared as a combined thermal event due to metastable eutectic melting, eutectic melting, and cocrystal (salt) melting and could not be resolved on the DSC curve. In total, eight physical mixtures showed signs of cocrystal or salt formation. The other 34 kinds of physical mixtures investigated showed DSC curves of a single endothermic peak. The DSC curves of physical mixtures of IND and either L-lysine or *o*-aminobenzoic acid are shown in Fig. 3 as examples of the results obtained from coformer screening.

The above eight physical mixtures that showed an exothermic peak, plural endothermic peaks, or a broad endothermic peak in the DSC curves were further analyzed using X-ray DSC. Diffraction peaks originated from cocrystals (salts) were detected in the X-ray DSC results of seven physical mixtures, with the one exception being the mixture of IND and meglumine. X-ray DSC results of the physical mixture of IND and saccharin are shown in Fig. 4.

Results of the coformer screening of IND were compared with those from a previous report (15). Our study was the first to note the presence of salts or cocrystals of IND and sorbic acid, *p*-toluenesulfonic acid, L-arginine, or L-lysine. A new cocrystal of IND and *o*-aminobenzoic acid was also found. In contrast, the cocrystal of IND and nicotinamide, which had been previously observed, was not detected in the present study (Table II). The DSC results of the physical mixture of IND and nicotinamide are shown in Fig. 5. The single endothermic peak appears as a typical DSC pattern of a physical mixture that is incapable of cocrystal formation. X-ray DSC was then conducted at a heating rate of 2°C/min, but no new diffraction peaks were detected. However, when X-ray DSC analysis was conducted at a slower heating rate of 1°C/min, new diffraction peaks did appear (Fig. 6), matching the

Table II Summary and Comparison of Screening Findings for Indomethacin

Name	pKa[a]	Thermal analysis method		Hit rate on slurry method (%)	Salt or cocrystal reported in a previous study (15)?
		DSC pattern	New diffraction peaks detected on X-ray DSC?		
L-arginine	13.6 (base)	Exothermic	Yes	13	No
L-lysine	10.6 (base)		Yes	100	No
Saccharin	1.6 (acid)		Yes	88	Yes
o-Aminobenzoic acid	4.9 (acid) 2.1 (base)	Plural endothermic	Yes	100	Not tested
p-Toluenesulfonic acid	−0.4 (acid)		Yes	25	No
Meglumine	9.2 (base)	Broad endothermic	No	50[c]	Yes
Sorbic acid	4.6 (acid)		Yes	88	No
Tromethamine	7.8 (base)		Yes	38	Yes
Nicotinamide	3.5 (base)	Simple endothermic	No[b]	75	Yes
Other 33 CCFs	–		Not tested	Not tested	Not tested

[a] Each pKa was calculated using ACD/Lab 2012. The pKa of indomethacin was 4.0 (acid)

[b] New diffraction peaks were detected at a heating rate of 1°C/min, but not 2°C/min

[c] Crystallinity of meglumine salt was very low

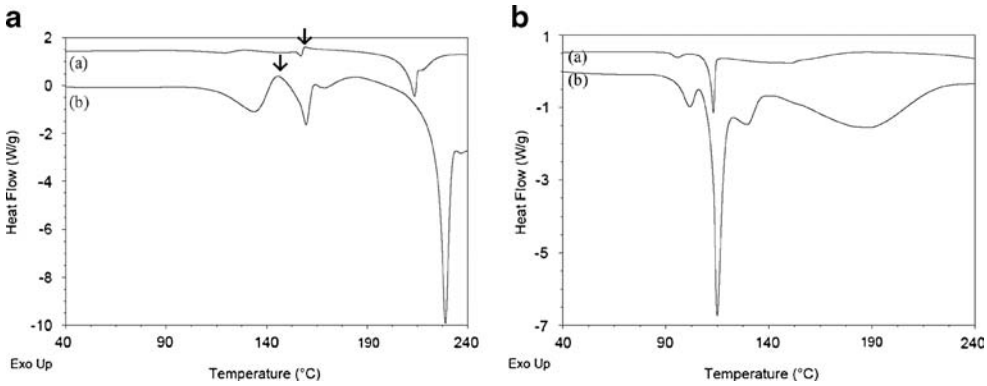

Fig. 3 DSC curves of a physical mixture of indomethacin and L-lysine (**a**) and indomethacin and *o*-aminobenzoic acid (**b**) upon coformer screening. Heating rates of (*a*) 5°C/min and (*b*) 30°C/min. *Arrows indicate* typical exothermic peaks.

diffraction peaks of the cocrystal of IND and nicotinamide (15). X-ray DSC results at 1°C/min indicated that the metastable eutectic temperature was approximately 103°C, with cocrystallization occurring at approximately 113°C (Fig. 6). Cocrystallization occurred in approximately 10 min after metastable eutectic melting. Therefore, regarding this mixture, relatively fast heating rates (more than 2°C/min) resulted in insufficient time for cocrystallization to occur between the metastable eutectic and cocrystal melting temperatures. In contrast, cocrystallization of a physical mixture of IND and saccharin occurred immediately after metastable eutectic melting at approximately 150°C (Fig. 4). Taken together, these results suggest that the kinetic barrier of IND and nicotinamide cocrystallization is higher and the nucleation of cocrystal is less likely in the supercooled melt state compared to other mixtures.

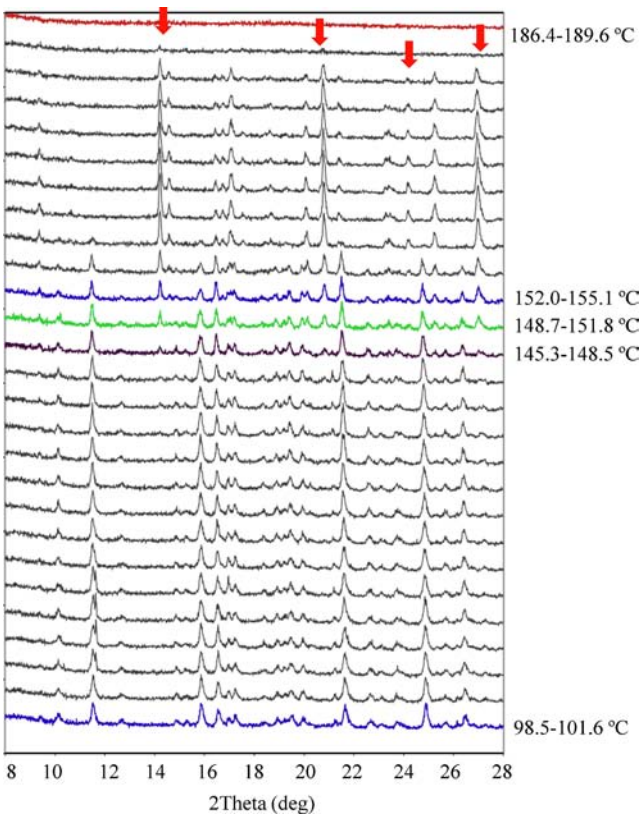

Fig. 4 X-ray DSC results of a physical mixture of indomethacin and saccharin obtained at a heating rate of 2°C/min. *Red arrows* indicates typical diffraction peaks of the cocrystal, which matched those shown in a reference (27).

Comparison of Thermal Analysis Method with Slurry Method on Indomethacin

To compare the detection capability of coformer screening between the thermal analysis and slurry methods, the latter was also conducted using IND and eight kinds of crystallization solvents. Nine kinds of coformers—namely tromethamine, meglumine, L-arginine, L-lysine, sorbic acid, *p*-toluenesulfonic acid, saccharin, nicotinemide, and *o*-aminobenzoic acid—were used based on the results of the thermal analysis method and a previous report (15). All cocrystals (salts) found via thermal analysis method were also obtained via the slurry method (Table III).

The hit rates, which were calculated by dividing the total number of wells where crystallization occurred by the number of solvents (eight), differed greatly depending on the coformers (Table II). While the IND and L-lysine salt or IND and *o*-aminobenzoic acid cocrystal formed easily regardless of the type of crystallizaiton solvent (100% hit rate), the hit rate of the IND and L-arginine salt or IND and *p*-toluenesulfonic acid cocrystal was markedly low (13% and 25%, respectively),

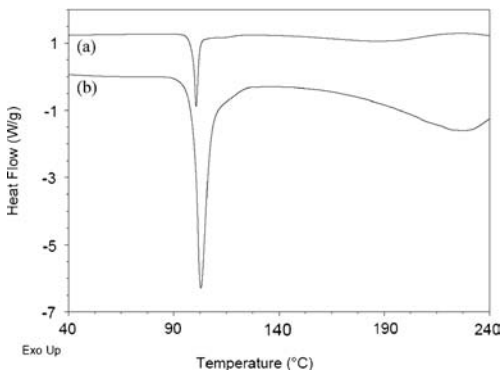

Fig. 5 DSC curves of a physical mixture of indomethacin and nicotinamide upon coformer screening. Heating rates of (**a**) 5°C/min and (**b**) 30°C/min.

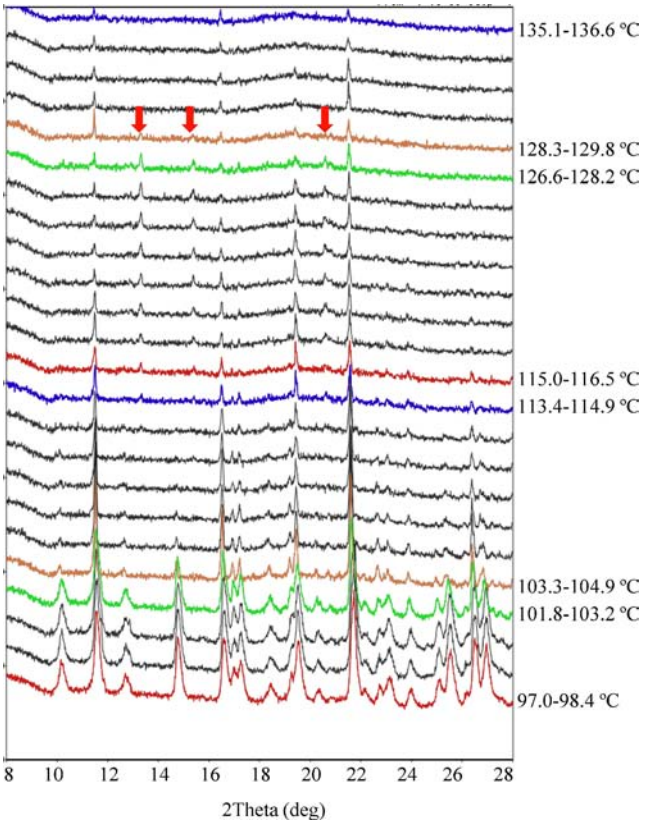

Fig. 6 X-ray DSC results of a physical mixture of indomethacin and nicotinamide obtained at a heating rate of 1 °C/min. *Red arrows* indicates typical diffraction peaks of the cocrystal, which matched those shown in a reference (15).

indicating that these salt and cocrystal may be elusive in the slurry method, because of the high dependency on the crystallization solvent. In fact, coformer screening of IND by the slurry method has been previously reported using only acetonitrile as a solvent and failed to observe the IND and L-arginine salt or IND and *p*-toluenesulfonic acid cocrystal (15). In contrast, IND and nicotinamide cocrystal were easily obtained (hit rate, 75%), which was not the case for the thermal analysis method. This relatively high hit rate indicates that the slurry method is more suitable than the thermal analysis method for the detection of IND and nicotinamide cocrystal, which has a high kinetic hindrance for cocrystallization and for which nucleation is difficult in the supercooled melt state.

Although the IND and meglumine salt was obtained in four different solvents via the slurry method, only a broad endothermic peak was detected in the DSC curve, and no new peaks were found using X-ray DSC analysis. As noted previously, the broad endothermic peak is considered to originate from a combined thermal event due to metastable eutectic melting, eutectic melting, and salt melting that could not be resolved on the DSC curve. One possible reason for our failure to identify the salt using X-ray DSC is that the diffraction peaks were too small to detect, as the crystallinity of the salt identified via the slurry method was extremely low.

Coformer Screening Using Thermal Analysis on Tenoxicam

Coformer screening based on thermal analysis was conducted using TEN as an alternative API model and 42 kinds of coformers. Exothermic peaks were detected on the DSC curves of physical mixtures of TEN with gentisic acid, maleic acid, malonic acid, *p*-aminobenzoic acid, and saccharin. The DSC curves obtained using the physical mixtures of TEN and

Table III Findings via the Slurry Method for Indomethacin

CCF	Solvent	1 Free	2 Tromethamine	3 Meglumine	4 L-arginine	5 L-lysine	6 Sorbic acid	7 *p*-Tluenesulfonic acid	8 Saccharin	9 Nicotinamide	10 *o*-Aminobenzoic acid
A	Acetonitrile	fr I	Tro II	Meg	am	Lys	Sor		Sac	Nic I	Ami
B	Ethanol	am		am	am	Lys	Sor	Tos	Sac	Nic II	Ami
C	1,4-Dioxane	fr II		am	am	Lys	fr II		Sac	fr II	fr II
D	2-Butanone		Tro I	Meg	am	Lys	am		Sac	Nic II	Ami
E	Ethyl acetate		Tro I	Meg	am	Lys	Sor		Sac	Nic II	Ami
F	Toluene	fr II	Tro I	Meg	am	Lys	Sor		Sac	Nic I	Ami
G	2-Propanol/H_2O (9:1)	fr I			Arg	Lys	Sor	Tos	Sac	Nic I	Ami
H	Tetrahydrofuran/ H_2O (9:1)	fr II				Lys	fr II				fr II

fr I free (γ, initial), *fr II* free (α, methastable), *Tro I* tromethamine salt-1, *Tro II* tromethamine salt-2, *Meg* meglumine salt (low crystallinity), *Arg* L-arginine salt, *Lys* L-lysine salt, *Sor* sorbic acid cocrystal, *Tos p*-toluenesulfonic acid cocrystal, *Sac* saccharin cocrystal, *Nic I* nicotinamide cocrystal-1, *Nic II* nicotinamide cocrystal-2, *Ami o*-aminobenzoic acid cocrystal, *am* amorphous, *blank columns* no powders

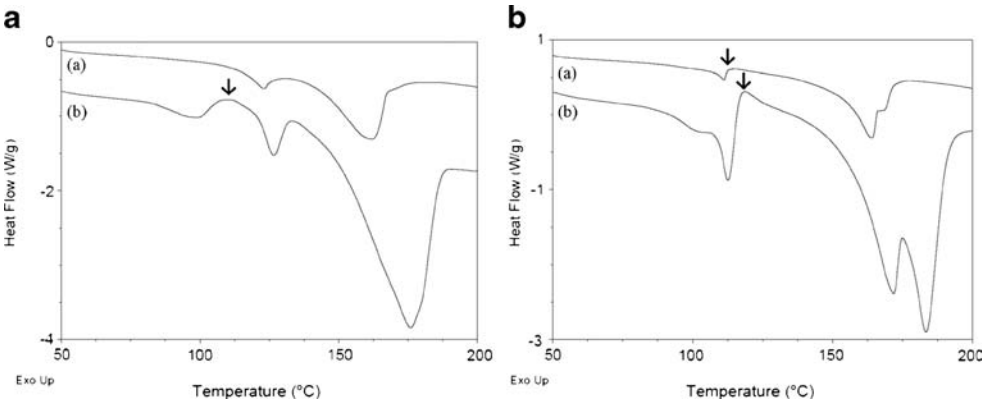

Fig. 7 DSC curves of a physical mixture of tenoxicam and maleic acid (**a**) and tenoxicam and malonic acid (**b**) upon coformer screening. Heating rates of (*a*) 5°C/min and (*b*) 30°C/min. *Arrows indicate* typical exothermic peaks.

malonic and maleic acid are shown in Fig. 7. Multiple endothermic peaks were found for the mixture of TEN and succinic acid, and a broad endothermic peak was found for the mixture of TEN and *p*-hydroxybenzoic acid (Table IV). Thus, seven physical mixtures showed signs of cocrystal or salt formation. The remaining 35 kinds of physical mixtures studied had DSC curves of a single endothermic peak.

The above seven physical mixtures that showed an exothermic, multiple endothermic, or a broad endothermic peak in the DSC curves were further analyzed using X-ray DSC. Diffraction peaks originating from the cocrystals (salts) were detected on X-ray DSC patterns for all of these physical mixtures.

The results of coformer screening of TEN were compared with those from a previous report (22). Similar to the IND results, we identified cocrystals of TEN and gentisic acid and TEN and *p*-aminobenzoic acid not previously seen; however, we failed to identify a cocrystal of TEN and glycolic acid which had been reported in the previous study (Table IV). The DSC curve was a single endothermic peak, indicating that the mixture is incapable of cocrystal formation (Fig. 8). Although X-ray DSC was conducted with a heating rate of 2°C/min, no new diffraction peaks were detected during the heating process. X-ray DSC analysis was also conducted at a slower heating rate of 1°C/min, but again, no diffraction peaks from the cocrystal of TEN and glycolic acid were found. TGA curves show that the total weight started to decrease due to the degradation of glycolic acid after metastable eutectic melting at approximately 76°C (Fig. 8), suggesting that the cocrystallization of TEN and glycolic acid failed to occur because of a loss of glycolic acid after metastable eutectic melting. This conclusion is reasonable, as glycolic acid alone

Table IV Summary and Comparison of Screening Findings for Tenoxicam

Name	pKa[a]	Thermal analysis method		Hit rate on slurry method (%)	Salt or cocrystal reported in a previous study (22)?
		DSC pattern	New diffraction peaks detected on X-ray DSC?		
Gentisic acid	3.0 (acid)	Exothermic	Yes	25	No
Maleic acid	2.4 (acid)		Yes	0	Yes
Malonic acid	2.9 (acid)		Yes	0	Yes
p-Aminobenzoic acid	4.9 (acid), 2.5 (base)		Yes	38[c]	Not tested
Saccharin	1.6 (acid)		Yes	100	Yes
Succinic acid	4.2 (acid)	Plural endothermic	Yes	0	Yes
p-Hydroxybenzoic acid	4.6 (acid)	Broad endothermic	Yes	0	Yes
Glycolic acid	3.7 (acid)	Simple endothermic	No[b]	0	Yes
Adipic acid	4.4 (acid)		No	0	No
Sorbic acid	4.6 (acid)		No	0	No
L-Tatraric acid	3.1 (acid)		No	0	No
Other 31 CCFs	–		Not tested	Not tested	Not tested

[a] Each pKa was calculated using ACD/Lab 2012. The pKa of tenoxicam was 4.5 (acid) and 3.5 (base)

[b] No new diffraction peaks were detected at a heating rate of 1 or 2°C/min

[c] Obtained as a mixture of free form and P-aminobenzoic acid cocrystal

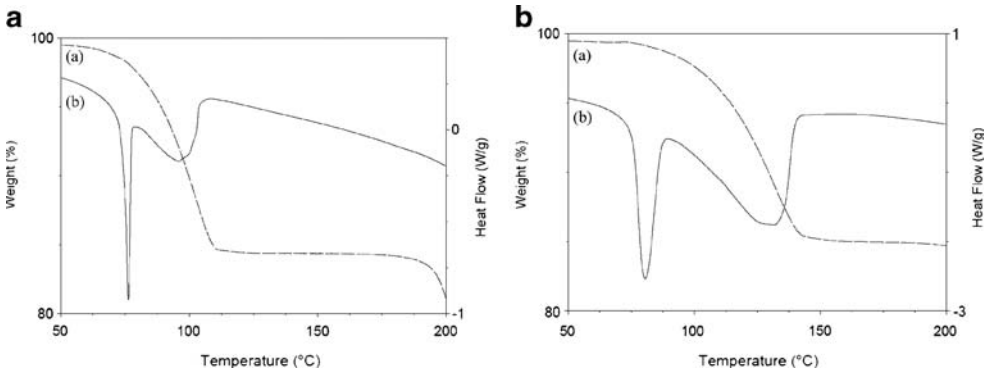

Fig. 8 Results of TGA (*a*) and DSC (*b*) of a physical mixture of tenoxicam and glycolic acid at heating rates of (**a**) 5°C/min and (**b**) 30°C/min.

is degraded soon after melting at approximately 79°C. In other words, degradation temperatures of glycolic acid in the melt were reached during the heating process before cocrystallization occurred. The potential concern when detecting cocrystal formation is therefore degradation of a compound near the metastable eutectic temperature.

In contrast, although maleic acid alone melts at approximately 132°C and degrades soon after (not shown), we found that TEN and maleic acid salt formed near the metastable eutectic temperature (approximately 100°C) and detected an exothermic peak (Fig. 7). Likewise, although malonic acid alone melts at approximately 136°C and degrades soon after (not shown), TEN and malonic acid cocrystals formed near the metastable eutectic temperature (approximately 115°C), with an exothermic peak detected (Fig. 7). These results indicate that degradation of a compound at the melting temperature, in itself, is not a matter of concern if an API and a coformer remain intact after metastable eutectic melting.

Comparison of Thermal Analysis and Slurry Methods on Tenoxicam

Coformer screening by the slurry method was conducted using TEN and eight kinds of crystallization solvents (Table V). Eleven kinds of coformers, including glycolic acid, *p*-hydroxybenzoic acid, succinic acid, maleic acid, manonic acid, saccharin, adipic acid, gentisic acid, sorbic acid, L-tartaric acid, and *p*-aminobenzoic acid, were examined, and the slurry method was compared with the thermal analysis method and a previous report (22). Only saccharin salts, gentisic acid cocrystals, and *p*-aminobenzoic acid cocrystals were obtained, with the *p*-aminobenzoic acid cocrystals found as a mixture of free form (Table V). In contrast, the TEN and maleic acid salt and cocrystals of TEN and malonic acid, succinic acid, and *p*-hydroxybenzoic acid, which were found by thermal analysis screening, were not obtained via the slurry method, and the free forms (initial form, form III, the most stable form) tended to precipitate. Additionally, solvates that contained acetonitrile, ethanol, or 1,4-dioxane, were obtained.

The hit rate of the screening by the slurry method is summarized in Table IV. The TEN and saccharin salt formed easily regardless of the crystallization solvent. While TEN and gentisic acid or *p*-aminobenzoic acid cocrystals were obtained using the slurry method screening, the hit rate was extremely low. Further, the hit rates of the TEN and maleic acid salt and TEN and malonic acid, succinic acid, *p*-hydroxybenzoic acid, and glycolic acid cocrystals were all 0%, a result likely due to the fact that TEN had extremely low solubility in organic solvents and a propensity to form solvates. The results of a simplified solubility test are shown in Table VI. The solubility of TEN in widely used crystallization solvents was almost less than 0.5 mg/mL and much lower than that of IND, suggesting differences in solubility between TEN and coformers were very large preventing cocrystallization in solution. Further, TEN formed solvates of acetonitrile, ethanol, and 1,4-dioxane, which also prevented cocrystallization from occurring. Coformer screening via the thermal analysis method was therefore superior to that of the slurry method for this API, which was characterized by low solubility and a propensity to form solvates. As the number of low-solubility APIs is increasing, the thermal analysis method will become all the more important for coformer screening.

Heat Generation Associated with Cocrystal (Salt) Formation

In a previous study (35), DSC was used for coformer screening while focusing only on heat absorption. In that study, a mixture of an API and coformer was determined to be capable of cocrystal formation when two endothermic peaks appeared at $T_{m\text{-}E}$ and T_c, but incapable if only a single endothermic peak appeared at T_E. In contrast, we used the observation of an exothermic peak being associated with cocrystal (salt) formation as the primary criterion to determine whether a mixture is capable of cocrystal (salt) formation. While a mixture incapable of cocrystal (salt) formation has no relationship with heat generation, one capable of cocrystal (salt) formation generates heat upon crystallization. Therefore the observation of heat can provide direct evidence for cocrystal (salt) formation. In

Table V Findings via the Slurry Method for Tenoxicam

CCF	Solvent	1 Free	2 Glycolic acid	3 *p*-Hydroxybenzoic acid	4 Succinic acid	5 Maleic acid	6 Malonic acid	7 Saccharin	8 Adipic acid	9 Gentisic acid	10 Sorbic acid	11 L-tartaric acid	12 *p*-Aminobenzoic acid
A	Acetonitrile	MeCN	MeCN	MeCN	MeCN	MeCN	MeCN	Sac	MeCN	Gen	MeCN	MeCN	MeCN
B	Ethanol	fr	EtOH	EtOH	fr	EtOH	fr	Mix I	EtOH	fr	fr	fr	fr
C	1,4-Dioxane	fr	fr	fr	Dio	fr	Dio	Sac	fr	fr	fr	fr	fr
D	2-Butanone	fr	fr	fr	fr	fr	fr	Sac	fr	fr	fr	fr	fr
E	Ethyl acetate	fr	fr	fr	fr	fr	fr	Sac	fr	Gen	fr	fr	Mix II
F	Toluene	fr	fr	fr	fr	fr	fr	Mix I	fr	fr	fr	fr	Mix II
G	2-Propanol/H_2O (9:1)	fr	fr	fr	fr	fr	fr	Mix I	fr	fr	fr	fr	Mix II
H	Tetrahydrofuran/H_2O (9:1)	fr	fr	fr	fr	fr	fr	Sac	fr	fr	fr	fr	fr

fr free form (initial, form III), *MeCN* acetonitrile solvate, *EtOH* ethanol solvate, *Dio* 1,4-Dioxane solvate, *Sac* saccharin salt, *Mix I* mixture of saccahrin salt and free, *Gen* gentisic acid cocrystal, *Mix II* mixture of *p*-aminobenzoic acid cocrystal and free

our study, the observation of two or more endothermic peaks is used as a secondary criterion for cocrystal (salt) formation. However, even in a mixture incapable of crystal (salt) formation, gradual heat absorption following eutectic melting often appears as a single peak, causing false positives. We therefore applied X-ray DSC as a secondary screening for those mixtures for which primary screening does not provide a decisive conclusion, further enhancing the credibility of the analysis.

Thermal Analysis Method in Terms of Drug Discovery Practice

The screening of 42 kinds of coformer was conducted using 0.42 g API within a week's time and should satisfy the demand of drug discovery practice. It should be emphasized that actual manual labor time was much less than a week because all instrumentation was automated, including grinding by the ball mill, weighing by a powder dispenser, and DSC measurements by an auto-sampler. The automation of this method was considered to be a large advantage compared with other screening methods, which need manual preparation and the removal of many solvents.

Table VI Solubility of Tenoxicam and Indomethacin

Solvent name	Solubility (mg/mL)	
	Tenoxicam	Indomethacin
Methanol	<0.5	10–20
Ethanol	<0.5	10–20
Isopropanol	<0.5	5–10
Acetonitrile	0.5–1	10–20
1,4-Dioxane	<0.5	>50
2-butanone	<0.5	>50
Ethy lacetate	<0.5	20–50
Tetrahydrofuran	<0.5	>50
Anisol	<0.5	10–20
Nitroethane	0.5–1	10–20
Toluene	<0.5	2–5
Isopropyl ether	<0.5	1–2
Water	<0.5	<0.5

In previous reports, grinding by a ball mill was generally conducted on a larger scale and required either or both more time or sample amount than would be available in the drug discovery stage. In our method, a combination of powder dispensing by automated robotics with grinding by the ball mill contributed to making the sample preparation efficient and of high throughput. In this study, the grinding conditions of a physical mixture were set for 5 min at 20/s frequency to prepare fine particles and mix them uniformly. However, the conditions of the ball mill still need to be optimized. When mixing and grinding particles of a physical mixture is insufficient, the thermal behavior of the mixture does not conform to the binary phase diagrams, as demonstrated in our previous report (24). In contrast, when materials are over-ground, the crystals of either or both the API and coformer become amorphous. In this case, crystallization of a single component might occur and give rise to an exothermic peak originating from the crystallization of the single component in the DSC analysis, which risks a false positive result. Although crystallization of the amorphous component rarely occurs in the DSC analysis and X-ray DSC is a powerful tool for identifying authentic diffraction peaks due to cocrystal (salt) formation, it is desirable to avoid the occurrence of misleading crystallization of single components.

Our previous study (24) clarified that diversity of the heating rate was essential for detecting peaks on DSC traces based on binary phase diagrams. Although heating rates of 5 and 30°C/min were adopted here to maintain a balance

between throughput and diversity in this study, faster heating rates could further improve detection sensitivity and screening efficiency. Optimization of the operating conditions for best coformer screening will be sought in future studies.

CONCLUSION

Novel coformer screening of salts and cocrystals based on binary phase diagrams using thermal analysis was conducted using indomethacin (IND) and tenoxicam (TEN) as model APIs and 42 kinds of coformers, with focus given to the exothermic and plural endothermic peaks of the DSC curves. The thermal analysis method is a high performance screening system, particularly for APIs such as TEN, which have low solubility in organic solvents and/or which form solvates in the slurry method. However, this thermal analysis method faces hurdles when used to examine APIs and coformers that show kinetic hindrance for the formation of salts or cocrystals during heating (e.g. IND and nicotinamide) or degrade near the metastable eutectic temperature (TEN and glycolic acid). Therefore the thermal analysis method and slurry method should be considered as complementary for coformer screening. Feasibility of the thermal analysis method in the drug discovery stage is ensured because of its small scale and high throughput. Given the increasing number of drug candidates which are insoluble in organic solvent, the thermal analysis method will prove quite useful in drug discovery practice given its lack of requirements for solvent, which also contributes to green chemistry.

ACKNOWLEDGMENTS AND DISCLOSURES

We thank Mayuko Mirun for assisting with the experiments.

REFERENCES

1. Aakeroy CB, Forbes S, Desper J. Using cocrystals to systematically modulate aqueous solubility and melting behavior of an anticancer drug. J Am Chem Soc. 2009;131(47):17048–9.
2. Remenar JF, Morissette SL, Peterson ML, Moulton B, MacPhee JM, Guzman HR, *et al.* Crystal engineering of novel cocrystals of a triazole drug with 1,4-dicarboxylic acids. J Am Chem Soc. 2003;125(28):8456–7.
3. Good DJ, Rodriguez-Hornedo N. Solubility advantage of pharmaceutical cocrystals. Cryst Growth Des. 2009;9(5):2252–64.
4. Trask AV, Motherwell WDS, Jones W. Physical stability enhancement of theophylline via cocrystallization. Int J Pharm. 2006;320(1–2):114–23.
5. Trask AV, Motherwell WDS, Jones W. Pharmaceutical cocrystallization: engineering a remedy for caffeine hydration. Cryst Growth Des. 2005;5(3):1013–21.
6. Karki S, Friscic T, Fabian L, Laity PR, Day GM, Jones W. Improving mechanical properties of crystalline solids by cocrystal formation: new compressible forms of paracetamol. Adv Mater. 2009;21(38–39):3905–9.
7. Sun CC, Hou H. Improving mechanical properties of caffeine and methyl gallate crystals by cocrystallization. Cryst Growth Des. 2008;8(5):1575–9.
8. McNamara DP, Childs SL, Giordano J, Iarriccio A, Cassidy J, Shet MS, *et al.* Use of a glutaric acid cocrystal to improve oral bioavailability of a low solubility API. Pharm Res. 2006;23(8):1888–97.
9. Tahara A, Kurosaki E, Yokono M, Yamajuku D, Kihara R, Hayashizaki Y, *et al.* Antidiabetic effects of SGLT2-selective inhibitor ipragliflozin in streptozotocin-nicotinamide-induced mildly diabetic mice. J Pharmacol Sci. 2012;120(1):36–44.
10. Mascitti V, Thuma BA, Smith AC, Robinson RP, Brandt T, Kalgutkar AS, *et al.* On the importance of synthetic organic chemistry in drug discovery: reflections on the discovery of antidiabetic agent ertugliflozin. MedChemComm. 2013;4(1):101–11.
11. Jones W, Motherwell S, Trask AV. Pharmaceutical cocrystals: an emerging approach to physical property enhancement. MRS Bull. 2006;31(11):875–9.
12. Stahly GP. Diversity in single- and multiple-component crystals. The search for and prevalence of polymorphs and cocrystals. Cryst Growth Des. 2007;7(6):1007–26.
13. Zhang GGZ, Henry RF, Borchardt TB, Lou XC. Efficient co-crystal screening using solution-mediated phase transformation. J Pharm Sci-Us. 2007;96(5):990–5.
14. Takata N, Shiraki K, Takano R, Hayashi Y, Terada K. Cocrystal screening of stanolone and mestanolone using slurry crystallization. Cryst Growth Des. 2008;8(8):3032–7.
15. Kojima T, Tsutsumi S, Yamamoto K, Ikeda Y, Moriwaki T. High-throughput cocrystal slurry screening by use of in situ Raman microscopy and multi-well plate. Int J Pharm. 2010;399(1–2):52–9.
16. Friscic T, Childs SL, Rizvi SAA, Jones W. The role of solvent in mechanochemical and sonochemical cocrystal formation: a solubility-based approach for predicting cocrystallisation outcome. CrystEngComm. 2009;11(3):418–26.
17. Weyna DR, Shattock T, Vishweshwar P, Zaworotko MJ. Synthesis and structural characterization of cocrystals and pharmaceutical cocrystals: mechanochemistry vs slow evaporation from solution. Cryst Growth Des. 2009;9(2):1106–23.
18. Padrela L, Rodrigues MA, Velaga SP, Fernandes AC, Matos HA, de Azevedo EG. Screening for pharmaceutical cocrystals using the supercritical fluid enhanced atomization process. J Supercrit Fluids. 2010;53(1–3):156–64.
19. Li ZB, Yang BS, Jiang M, Eriksson M, Spinelli E, Yee N, *et al.* A practical solid form screen approach to identify a pharmaceutical glutaric acid cocrystal for development. Org Process Res Dev. 2009;13(6):1307–14.
20. Karki S, Friscic T, Jones W, Motherwell WDS. Screening for pharmaceutical cocrystal hydrates via neat and liquid-assisted grinding. Mol Pharm. 2007;4(3):347–54.
21. Bysouth SR, Bis JA, Igo D. Cocrystallization via planetary milling: enhancing throughput of solid-state screening methods. Int J Pharm. 2011;411(1–2):169–71.
22. Patel JR, Carlton RA, Needham TE, Chichester CO, Vogt FG. Preparation, structural analysis, and properties of tenoxicam cocrystals. Int J Pharm. 2012;436(1–2):685–706.
23. Berry DJ, Seaton CC, Clegg W, Harrington RW, Coles SJ, Horton PN, *et al.* Applying hot-stage microscopy to co-crystal screening: a study of nicotinamide with seven active pharmaceutical ingredients. Cryst Growth Des. 2008;8(5):1697–712.
24. Yamashita H, Hirakura Y, Yuda M, Teramura T, Terada K. Detection of cocrystal formation based on binary phase diagrams using thermal analysis. Pharm Res. 2013;30(1):70–80.

25. Cooke CL, Davey RJ, Black S, Muryn C, Pritchard RG. Binary and ternary phase diagrams as routes to salt discovery ephedrine and pimelic acid. Cryst Growth Des. 2010;10(12):5270–8.
26. Alleso M, Velaga S, Alhalaweh A, Cornett C, Rasmussen MA, van den Berg F, *et al.* Near-infrared spectroscopy for cocrystal screening. A comparative study with Raman spectroscopy. Anal Chem. 2008;80(20):7755–64.
27. Basavoju S, Bostrom D, Velaga SP. Indomethacin-saccharin cocrystal: design, synthesis and preliminary pharmaceutical characterization. Pharm Res. 2008;25(3):530–41.
28. Umeda Y, Fukami T, Furuishi T, Suzuki T, Tanjoh K, Tomono K. Characterization of multicomponent crystal formed between indomethacin and lidocaine. Drug Dev Ind Pharm. 2009;35(7):843–51.
29. Cantera RG, Leza MG, Bachiller CM. Solid phases of tenoxicam. J Pharm Sci-Us. 2002;91(10):2240–51.
30. Wouters J. Pharmaceutical salts and co-crystals. Cambridge: The Royal Society of Chemistry; 2012.
31. Database of Select Committee on GRAS Substances (SCOGS) Reviews. Available from: http://www.fda.gov/Food/IngredientsPackagingLabeling/GRAS/SCOGS/ucm084104.htm.
32. Stahl PH, Wermuth, Camille G. Handbook of pharmaceutical salts. 2nd ed. Weinheim: WILEY-VCH Verlag GmbH; 2011.
33. Nygren CL, Wilson CC, Turner JFC. Electron and nuclear positions in the short hydrogen bond in urotropine-N-oxide-formic acid. J Phys Chem A. 2005;109(9):1911–9.
34. Aakeroy CB, Fasulo ME, Desper J. Cocrystal or salt: does it really matter? Mol Pharm. 2007;4(3):317–22.
35. Lu E, Rodriguez-Hornedo N, Suryanarayanan R. A rapid thermal method for cocrystal screening. Crystengcomm. 2008;10(6):665–8.